DM aperture operating in its Classical Lyot Coronagraph (CLC) mode (Fig. 3). These results are 4× better in contrast and 1.6× better in IWA than we had previously achieved for a monolithic test aperture in 2020. Critically, HiCAT has yielded experimental validation of sensing and software methods for continuous contrast maintenance on segments [Pourcelot et al., 2022]. For instance, when operating with a PAPLC in a closed loop with Zernike LOWFS, HiCAT routinely achieves contrasts of 2×10^{-8} over $2 - 13\lambda/D$ and 9×10^{-9} over $5 - 13\lambda/D$. HiCAT has also demonstrated continuous maintenance using science images to stabilize contrast at 3×10^{-8}, operating at 1 Hz under large synthetic drifts injected with our DM primary surrogate [Redmond et al., 2022]. These contrast and IWA milestones satisfy the goals of our previous APRA and SAT programs in monochromatic light, with broadband demonstrations to be completed in 2023.

4. Technical Approach and Methodology

4.1. **ASSIST requirements for system-level TRL-5 demonstration of contrast maintenance.** The top-level requirements for ASSIST flow down from the performance needed to enable a system-level demonstration at TRL-5. We adopt an off-axis design following Astro2020. The concave, off-axis primary is followed by a convex secondary, and then a tertiary to inject the beam into the coronagraph. While IROUV will most likely use a three-mirror anastigmat design for wide field performance, a simpler Cassegrain design is sufficient for coronagraph demonstrations. The primary's focal ratio should be close to the $\sim$ f/3 primary envisioned for LUVOIR B. Fig. 4 shows a conceptual view of the full ASSIST bench on top of the existing HiCAT-1 coronagraph, assuming a 25 cm primary (i.e. about the maximum size we would consider).

To co-phase the segments, and to inject intentional drifts for system-level contrast maintenance tests, the primary will require both coarse and fine range adjustment capabilities. The primary mirror diameter should be in the range $10 - 25$ cm, so that the overall ASSIST subsystem is small enough to integrate with high-contrast testbeds in a vacuum tank, and yet large enough for both coarse and fine actuation hardware, as well as temperature sensors, or future upgrade with edge sensors or laser metrology. To allow integration and alignment, and operation prior to integration with a coronagraph testbed, there must be space for an imaging camera and wavefront sensor (e.g. the mid-order wavefront sensor looking at the telescope aperture, as envisioned in the LUVOIR control architecture.) The design should be sufficiently general to be replicated cost-effectively for multiple testbeds in the future.

The system must achieve sufficient stability in vacuum to enable tests at 10^{-10} contrast, though operating at the faster timescales enabled by bright lab light sources as explained above in 2.2. Stability of order $\sim$ 300 pm/s would suffice. It is important to note that the technology need motivating this APRA is focused on high-contrast dark zone control algorithms and stability. We are not developing flight technology for the telescope itself, and the segments and actuators need not have flight traceable designs. Nor is it needed in this context to consider an initial alignment task comparable to the optical commissioning of JWST, which is now at TRL-9.

4.2. **Prototyping methodology for static demonstration, completed under IRAD.** Design and prototyping work started in 2018 using funding competitively awarded by the STScI Director's Discretionary Fund. The goal was to establish a practical path to build a segmented mirror meeting the above requirements, including parabolic segment fabrication, assembly process, and opto-mechanical actuation with continuous capture ranges from the post-assembly mechanical tolerances all the way down to sub-nanometer resolution. The design budget targets $\sim$ 7.5 nm RMS surface error. Iterative development was carried out by our team, including three cohorts of JHU mechanical engineering undergrads and grad students.

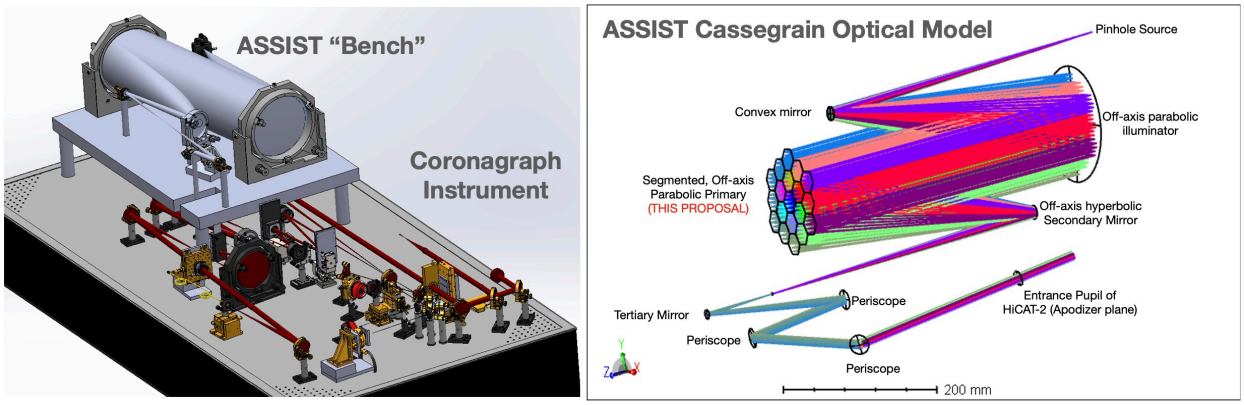

FIGURE 4. **Left:** Concept-view of an ASSIST telescope bench on top of a coronagraph. Here the 4'x8' HiCAT-1 is shown as a placeholder for HiCAT-2; the ASSIST bench is notionally 2'x3'. **Right:** Preliminary ASSIST design, including Cassegrain illuminator and telescope (f/3 off-axis parabolic segmented primary mirror, hyperbolic secondary, collimating tertiary, and periscope for beam injection into the coronagraph).

We identified key trades and design decisions (summarized in Fig. 5), and assessed them through extensive mechanical modeling (CAD) and component-level fast prototyping (e.g to test alignment tolerances or actuator performance), to obtain multiple advanced prototypes. Those design trades and their results are as follows.

4.2.1. *Parabolic segment manufacturing, cutting, and segment gap control.* We investigated several approaches to segment manufacturing and identified two viable options. Student-led work included assembly and metrology on several prototypes to test gaps, and adhesives. In addition to very high segment surface quality ($\sim \lambda/100$ surface RMS), gaps must have minimal roll-off and be $\lesssim 1\%$ of the segment size [Shaklan et al., 2019, Bolcar et al., 2017]. Given our target segment size of $\sim 2-3$ cm, we aim for 250 µm gaps.

◦ Our baseline method cuts segments from a monolithic primary parent mirror. However, high-quality cuts are much wider than our gaps, which means cutting "into" adjacent segments, thus wasting part of the glass. The most efficient pattern of cuts requires three monolithic mirrors to generate a complete set of segments for a single primary. Thus, we will harvest three Off-axis Parabolas (OAP) from a large mother parabola ($\sim$ 400 mm diameter), then section each OAP into hexagons. We tested this by cutting three off-the-shelf parabolic (on-axis) f/4 mirrors to create our 19-segment parabolic prototype[2], and aligning the segments via steps similar to JWST commissioning (Fig. 6). This cutting process demonstrated sufficient precision for our alignment budgets.
◦ A second method, developed by our collaborators in Marseille, uses stress polishing. This method was used for some HiCAT super-polished mirrors and for Roman Coronagraph OAPs [Caillat et al., 2022]. This will involve polishing a "solid block" of flat segments bonded together on a deformation harness. After a spherical polish and segments release by chemical attack, they take the OAP shape. Under STScI-IRAD and CNES co-funding, Marseille will deliver a 7-segment prototype in 2023, which we plan to test in our first year mirror prototype as part of this APRA.

4.2.2. *Assembly and bonding.* We tested several variants for bonding segments to actuators, including transferring the bonded polished segments as a "solid block" to the actuated backplane

[2]This method it not applicable for IROUV itself, and limited to small mirrors ($\lesssim$ 20 cm.)

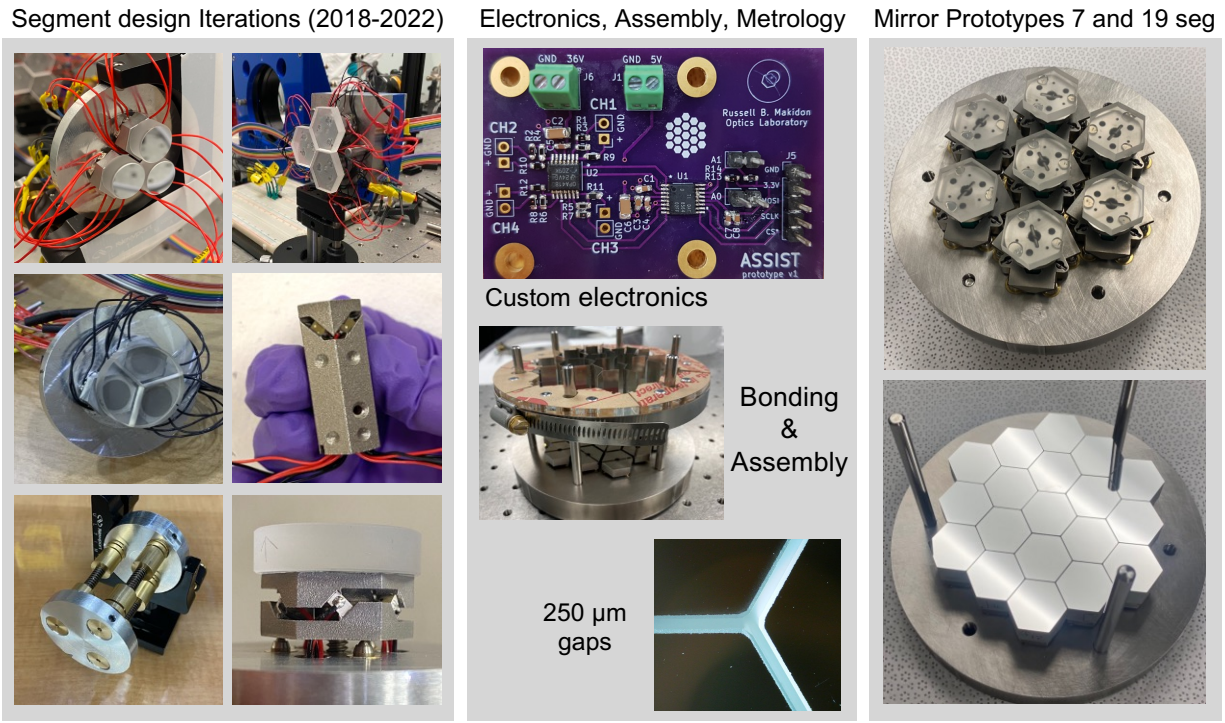

FIGURE 5. Highlights of our IRAD-funded maturation of a segmented primary mirror since 2018, performed by $\sim$ 15 undergraduate students. Hardware prototypes included flexure-based Stewart platforms, differential screws designs, piston/tip/tilt stages, and various combinations of coarse and fine actuation with 3 and 6 degrees of freedom. Two complete mirror prototypes were completed recently to measure performances: 1) a flat 7 segment (top right) to test 6 DoF coarse actuation with 3 DoF fine piezo stage and their capture range overlap; 2) a parabolic 19 segment (bottom right) with 3 DoF coarse to demonstrate segment fabrication, assembly, gap quality statistics, and coarse capture ranges and resolution.

and releasing them on-site. As part of that, we investigated custom-formulated adhesives to optimize mechanical and thermal properties, curing time, and ability to differentiate permanent from temporary adhesives. We ultimately selected a contact metrology approach with shims between segments held by a custom jig (Fig. 5 center). This method achieved excellent gap quality and uniformity. We measured all the gaps on our 19-segment prototype using a measuring microscope with $\sim$ 2 µm accuracy. Using 254 µm shims, we obtained mean = 264 µm and standard deviation = 14 µm for the bonded mirror gaps, meeting the necessary tolerances.

4.2.3. *6 vs. 3 degrees of freedom coarse actuation designs.* Each segment needs active control with very fine accuracy (sub-nanometer) in piston, tip, and tilt (P/T/T). These three *strong* DoFs require finer resolution because their misalignment impact is far larger than those from the other 3 DoFs: radial and azimuthal translation, and clocking. We assessed the desirable simplification to also limit coarse actuation to 3 DoF. This depends on the optical design speed (f-number), and on the manufacturing and positioning tolerances. We tackled this issue both using optical modeling and hardware prototype validation.

We developed a complete ASSIST optical design (Fig. 4) and investigated the sensitivity to the 6 DoF modes of a f/3 primary (this faster primary is most stressing, as tolerances relax for slower optics). Monte Carlo modeling, assuming initial random segment misaligmnents with a range of +/- 0.2 mm followed by P/T/T compensation, yielded an average wavefront error of 15 nm RMS

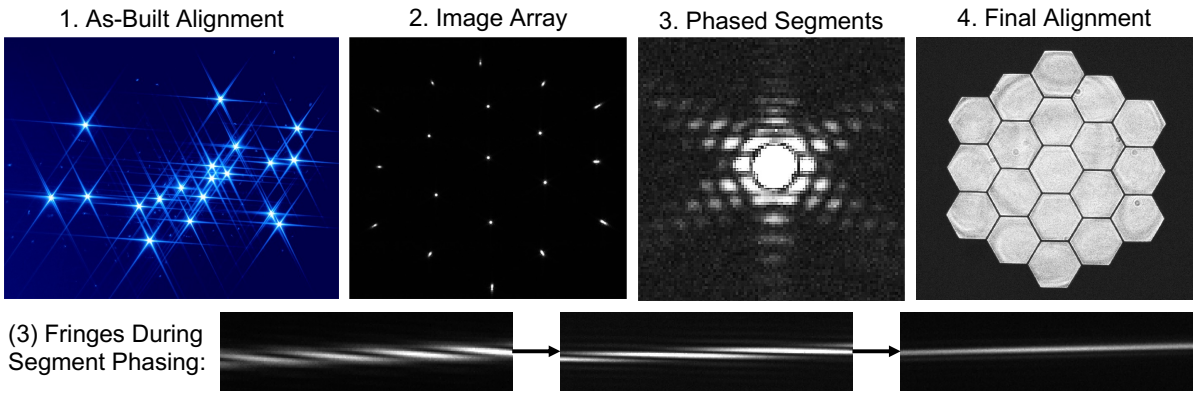

FIGURE 6. We have aligned the 19-segment prototype in stages similar to JWST commissioning in early 2022. (1): Initial image showing 19 scattered images from initial tip/tilt errors after bonding and assembly. (2): An image array created after identifying each segment image to begin the alignment and stacking process. (3): two segments stacked and fully phased in piston, with accompanying dispersed fringes used during the process shown below, directly analogous to the dispersed Hartmann sensing method used with JWST. (4): Interferogram after complete alignment, showing good qualitative phasing relative to the interferometer's reference sphere. (Unfortunately a recent interferometer laser failure creates these low-contrast fringes that prevent quantitative measures until repaired.)

(i.e. 7.5 nm surface), with a range of $10-20$ nm over the Monte-Carlo run. Therefore, 3 DoF coarse mounts are sufficient to meet alignment needs, which reduces complexity, cost, and risk.

In parallel, a rapid prototyping exercise pursued both 3 and 6 DoF designs options. The 6 DoF design serves as a contingency for a possible future ASSIST variant that may require it. 6 DoF mounts are typically obtained using Stewart Platforms (aka hexapods, as on JWST). Hexapods are however very difficult to integrate in a small package. We developed a novel mechanical approach to a 6-DOF coarse actuation design, where the stage remains extremely compact and possible to integrate with a 3 DoF piezo stage. This was successfully tested in a 7-segment prototype shown in the upper right of Fig. 5. Using *coarse actuation* only on 7 flat segments with this 6 DOF mount (42 screws) we reached 53 nm RMS surface error, which vastly surpassed expectations.

4.2.4. *Coarse and fine range precision, ranges, and collision avoidance.* We selected piezoelectric actuators to achieve the necessary fine range precision. These piezos can be combined with strain gauge sensors (SGS) to circumvent hysteresis and stabilize their length in closed loop. Commercial solutions can deliver very small resolutions ($\sim$ 10 pm range), but these are expensive. We demonstrated that given our coarse accuracy (discussed next), we only need about 15V for fine range control (low-voltage electronics are desirable in terms of cost and stability). Our prototypes use custom electronics to save costs, most recently a low-voltage, low-resolution version for our latest 3-segment prototype with upcoming open-loop stability tests. We have baselined a complete commercial solution but will investigate alternatives in light of that result.

For coarse actuation, we adopt high thread-count screws (508 threads/inch). In our final-design 3-segment prototype, *using coarse actuation only* we reached 11 nm RMS surface error, well within the fine range envelope of the piezos. Based on our measured resolution with a single coarse actuator ($<$ 1 µm), we calculated a coarse tip-tilt resolution of 110 µrad. The full range of fine tip-tilt motion is 1300 µrad, providing coarse/fine tip-tilt range overlap by a factor of $\sim$ 12.

On the 19-segment prototype, we measured the pre-alignment installation tip/tilt error to be 5.7 mrad. Assuming a 100% solid-body collision avoidance model in CAD, this corresponds to a

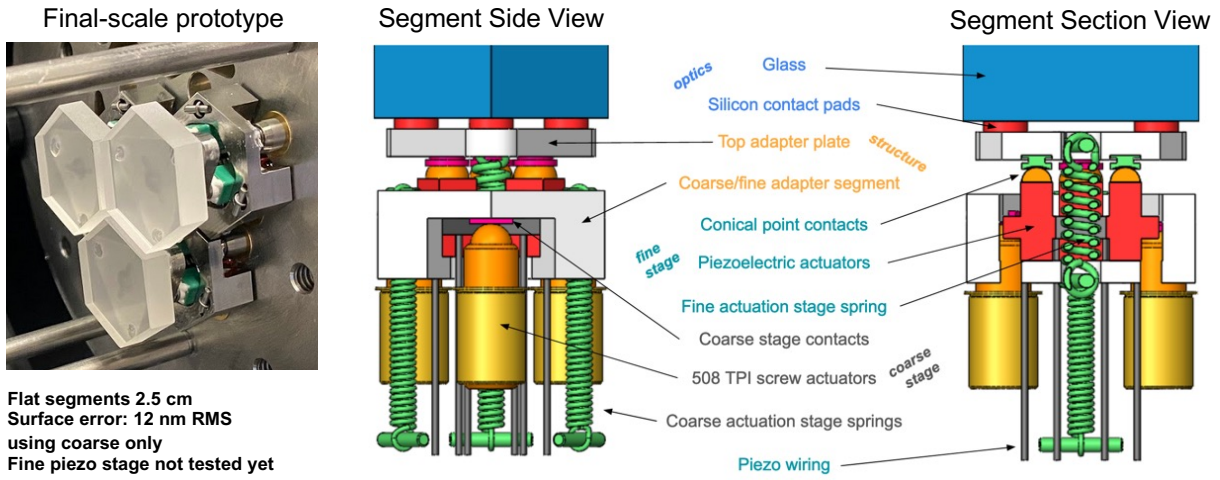

FIGURE 7. Latest, and most compact design informed by prototyping trade studies with ~ 2.7 cm segments corresponding to the proposed ~ 15 cm, 19-segment mirror (size and configuration may still change slightly). The coarse stage uses high thread-count screws in contact with a stainless steel adapter plate. The fine stage uses ball and conic contacts on preloaded piezos. The assembly is entirely modular: both coarse and fine stages, and glass can be disassembled by removing the springs pins. Side bonding and similar materials are used to minimize thermal expansion effects, and components are vacuum-compatible. This prototype has reached 11.6 nm RMS surface alignment with flat segments (2.54 cm) using coarse control only; the fine control is pending completion and test of the custom piezo electronics and we plan to perform a preliminary stability test at the GSFC Ultra-Stable Structures lab in air.

factor of safety of ~ 2 for collision avoidance after the coarse tip/tilt actuation. Initial coarse piston errors are not an issue at all, since the screws have > 1 mm range. We will continue to refine our assembly process (including bonding tests and metrology) to increase this figure of safety, and if necessary can also readily debond the segments and try again before our 7-segment prototype.

4.2.5. *Number and size of segments.* Number is a free parameter and not critical. A future version of ASSIST could be scaled straightforwardly to match whatever aperture geometry is eventually adopted for IROUV. But the hardware cost for mechanisms and electronics scales roughly with the number of segments. For current needs, 19 segments is a practical choice that provides sufficient degrees of freedom to represent a complex segmented telescope, while keeping project costs lower compared to larger segment counts (e.g. cost lower by $\sim 50\%$ compared to 37 segments for the next size up). Size is a big cost driver because of glass manufacturing, and likely a driver on stability. Thus, we have produced the most compact design given all these constraints.

4.2.6. *Final design and preliminary stability testing.* Based on these results, we refined a segment design at the correct form-factor for the complete ~ 15 cm 19-segment mirror we propose to build. It incorporates 3 DoF coarse + 3 DoF fine controls, relying on manufacturing, assembly tolerances, and compensation to control the weak 3 DoFs. A new 3-segment prototype of that design with custom electronics was completed recently (Fig. 7). This will be tested at GSFC in 2023 as a best-effort collaboration in air (still supported by IRAD) using their high-speed (kHz) interferometer. We hope to gain a factor $10\times$ or more compared to our Fizeau interferometer over long integrations. Our goal is to obtain preliminary stability upper limits before this work starts.

4.3. **Methodology for dynamic stability test of segmented primary mirror in vacuum.** To further test and characterize these mirrors in preparation for later high contrast demos we must proceed to vacuum. Our methodology for developing and testing first a 7-segment and then a 19-segment mirror will combine 3-D and finite element mechanical modeling, thermal modeling, and data from thermal instrumentation and wavefront stability measurements. We are teaming with the Ultra-Stable Structures Lab (USS) at GSFC [Saif et al., 2017, 2019a,b, Feinberg et al., 2022]. The USS lab is a facility to measure wavefront stability at the picometer level, developed over the past six years, and building on over a decade of work and expertise characterizing the stability of JWST mirrors [Saif et al., 2018]. Recent results have demonstrated the capability to control and detect surface RMS drift rates less than 3 pm/second [Feinberg et al., 2022]. This is 100× better than our requirement from Sec.2.2

4.3.1. *Thermal modeling and design optimization for vacuum and stability.* Based on IRAD-funded evaluation of static and preliminary dynamical results using our 3-segment prototype (Fig.7), a linear thermal distortion model of one segment will be used to inform design updates to build our 7-segment prototype. This thermal model will be further informed by data from multiple sensors installed on the mirror backplane, combined with wavefront stability measurements with the high-speed interferometer both under stable conditions and controlled thermal load. Data analyses and modeling tools will help us finalize the design of the 19-segment ASSIST primary mirror, with vacuum optimizations of components and adhesives. The model will be used during the final test campaign to understand the mirror's thermal and dynamic stability, which will in turn serve as an input to subsequent work on high-contrast dark hole stability modeling.

4.3.2. *Segmented mirror thermal stabilization and control.* We will investigate two possible ways to control and stabilize the mirror temperature. We will first adapt the current approach used at USS to stabilize the temperature of mirror test articles using radiative transfer. This thermal control approach uses a heater plate immediately behind the mirror substrate and radiatively heats the substrate to stabilize its temperature. This method recently stabilized a mirror temperature at 25 deg C with a Peak-to-Valley variation of 250μK over 18 hours [Feinberg et al., 2022]. Our mirror is about the same size as the glass mirror tested at USS ($\sim$ 12 cm), so this technique and existing hardware should be readily adaptable.

Because our actuated mirror will have more localized thermal loads due to the piezo actuators, we will also investigate using multiple sensors and heaters for a more refined thermal control. This approach will also build on the experience and thermal control equipment available at the USS lab, as well as additional thermal sensors and controllers included in this proposal. *Such an approach would be closely analogous to localized thermal control envisioned for the IROUV flight system.*

4.3.3. *High stability data acquisition and processing.* We will use the USS high-speed interferometer in specular mode at 632 nm or 532 nm, since the mirrors will be coated. We will acquire data in a range from hundreds of Hertz to kHz. The rapid data acquisition system can register tens of thousands of wavefront data frames, which are then analyzed to increase the signal to noise. The temporal timescales for our long-term goal with ASSIST combined with a coronagraph instrument will include fast wavefront sensing using the science camera at 10-50 Hz, with control loops at 1-10 Hz and experiments of the order of 1000 s. Therefore, the USS temporal capabilities are well matched to explore the stability properties of segmented mirrors over the timescales of interest.

We will follow the same methodology as previously used by the USS team to test a commercial picometer actuator. We will test the mirror both under static conditions and under sinusoidal variations of a segment, after calibration of the amplitude response of the piezos. Given that the